Improvement of Dynamical Stability Using Interline Power Flow Controller

Mohamad Reza BANAEI, Abdel-Rahim KAMI
Electrical Engineering Department, Faculty of Engineering, Azarbaijan University of Tarbiat Moallem,
35 Km Tabriz-Marageh road, Tabriz, Iran
m.banaei@ azaruniv.edu

***Abstract*—This paper presents a novel linearized Phillips-Heffron model of a power system installed with an Interline Power Flow Controller (IPFC) in order to studying power system stability. In addition, a supplementary controller for a novel modeling IPFC to damp low frequency oscillations with considering four alternative damping controllers is proposed. In this paper selection of effectiveness damping control signal for the design of robust IPFC damping controller to variations in system loading and fault in the power system are discussed. The presented control scheme not only performs damping oscillations but also the independent interline power flow control can be achieved. MATLAB simulation results verify the effectiveness of the IPFC and its control strategy to enhance dynamical stability.**

***Index Terms*—Power system dynamic stability, Phillips-Heffron model, Supplementary controller, IPFC**

I. INTRODUCTION

The recent interconnection between power systems and expansion in transmission and generation meant to satisfy the increasing power demand, thus, the dynamic stability of power systems became an important object in the great power systems stability. Power System Stabilizer (PSS) has been used as a simple, effective, and economical method to increase power system oscillation stability. While PSS may not be able to suppress oscillations resulting from severe disturbances, such as three phase faults at generator terminals [1], Flexible AC Transmission System (FACTS) controllers, such as Static Var Compensators (SVC), Static Synchronous Compensators (STATCOM), and Unified Power Flow Controller (UPFC), can be applied for damping oscillations and improve the small signal stability of power systems by adding a supplementary signal for main control loops [2-3].

Interline Power Flow Controller (IPFC) [4] is a new concept of the FACTS controller for series compensation with the unique capability of controlling power flow among multi-lines.

The IPFC employs two or more voltage source converters (VSCs) with a common dc-link. Each VSC can provide series compensation for the selected line of the transmission system (master or slave line) and it is capable of exchanging reactive power with its own transmission system.

The damping controller of low frequency oscillations in the power system must be designed for a nonlinear dynamic model of power system. But, because of the difficulty of this process, generally the linear dynamic model of the system at an operating point is put and controller design is analyzed. An obtained controller is investigated in the nonlinear dynamic model for its accuracy and desirable operation at damping of oscillation.

In [5], a linearized model of a system, with two IPFC lines installed, has worked, but a SSSC or STATCOM can be employed in the system with a single machine and two lines, out of economic reasons. The active or reactive power of the lines is not controlled independently.

In this paper, a connected single machine to infinite bus with three IPFC lines installed is used and a novel linearized Phillips-Heffron model for the mentioned power system is derived for design of the IPFC damping controller.

In order to enhance power system dynamical stability, a supplementary signal which is the same as that applied for other FACTS devices [6-9], is superimposed on the main input control signals. Next, the effect of IPFC damping controller on low frequency oscillations of power system is investigated. Four alternative IPFC based damping controllers are considered. Contribution of pure positive damping torque of the damping controllers are used to choose the most effective control signal of the IPFC to damp low frequency oscillations, the same as TCSC and UPFC [10, 12].

II. PROPOSED POWER SYSTEM INSTALLED WITH IPFC FOR DYNAMIC STABILITY STUDY

Figure 1 shows a single-machine infinite-bus power system installed with a IPFC which consists of a Master voltage source converter (VSC-M), a Slave voltage source converter (VSC-S) and its two transformers and a DC link capacitor (C_{dc}). V_{inj1}, V_{inj2} are voltages of transformers of line 1 and line 2 respectively. The infinite bus is supplied in parallel by three lines. Because of the third line in the power system and its free power flow, the active and reactive power flow on other lines are controlled independent of power flow of third line. While the system is utilized only with two lines, SSSC or STATCOM is installed for the purpose of power flow control and other control functions. In Fig. 1, $m_1, m_2, \delta_1, \delta_2$ are the amplitude modulation ratio and phase angle of the control signal of each VSC respectively, which are the input control signals to the IPFC and $V_b, V_s, v_{inj1}, v_{inj2}$ are the voltage of infinite bus, terminal voltage of generator and the injective voltages of the Master and slave voltage source converter respectively.

Digital Object Identifier 10.4316/AECE.2010.01007

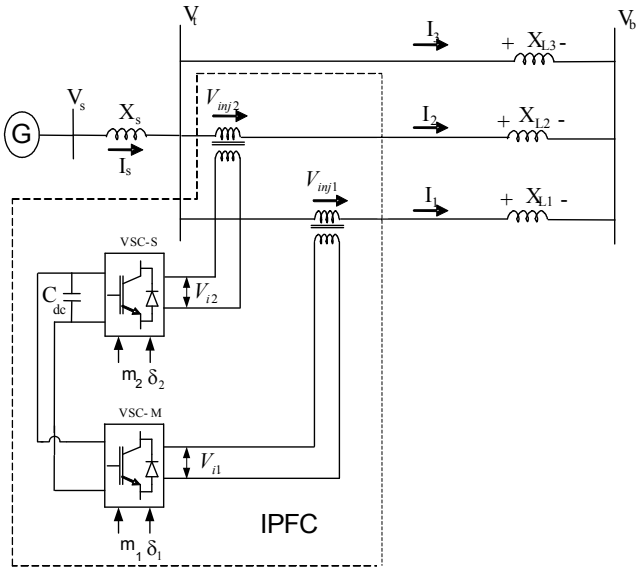

Figure 1. A single-machine infinite-bus power system installed with an IPFC.

III. Power System Non-Linear Model

The general pulse width modulation (PWM) (or optimized pulse patterns or space-vector modulation approach) is adopted for the IGBT-based VSC. By ignoring the resistance of the transformers of the IPFC and by applying Park's transformation, the per unit of three-phase dynamic differential equations of the IPFC as the three-phase dynamic differential equations of the UPFC [11] are obtained:

$$\begin{bmatrix} V_{inj\,1d} \\ V_{inj\,1q} \end{bmatrix} = \begin{bmatrix} 0 & X_{t1} \\ -X_{t1} & 0 \end{bmatrix} \begin{bmatrix} I_{1d} \\ I_{1q} \end{bmatrix} + \begin{bmatrix} V_{i1d} \\ V_{i1q} \end{bmatrix},$$
$$V_{i1d} = \frac{m_1 V_{dc} \cos \delta_1}{2}, \qquad (1)$$
$$V_{i1q} = \frac{m_1 V_{dc} \sin \delta_1}{2}$$

$$\begin{bmatrix} V_{inj\,2d} \\ V_{inj\,2q} \end{bmatrix} = \begin{bmatrix} 0 & X_{t2} \\ -X_{t2} & 0 \end{bmatrix} \begin{bmatrix} I_{2d} \\ I_{2q} \end{bmatrix} + \begin{bmatrix} V_{i2d} \\ V_{i2q} \end{bmatrix},$$
$$V_{i2d} = \frac{m_2 V_{dc} \cos \delta_2}{2}, \qquad (2)$$
$$V_{i2q} = \frac{m_2 V_{dc} \sin \delta_2}{2}$$

$$\frac{dv_{dc}}{dt} = \frac{m_1}{2C_{dc}} \begin{bmatrix} \cos \delta_1 & \sin \delta_1 \end{bmatrix} \begin{bmatrix} I_{1d} \\ I_{1q} \end{bmatrix} + \frac{m_2}{2C_{dc}} \begin{bmatrix} \cos \delta_2 & \sin \delta_2 \end{bmatrix} \begin{bmatrix} I_{2d} \\ I_{2q} \end{bmatrix} \qquad (3)$$

where X_{t1}, X_{t2} are the reactance of master and slave injection transformers and v_{dc} is the DC link voltage and, $\bar{I}_1 = I_{1d} + jI_{1q}$, $\bar{I}_2 = I_{2d} + jI_{2q}$.

The complete dynamic model of a single-machine infinite-bus power system equipped with an IPFC can be developed by combining (1-3) with the machine dynamic equations shown below:

$$\begin{aligned} \dot{\delta} &= \omega_0 \omega \\ \dot{\omega} &= \left(P_m - P_e - D\omega\right)/2H \\ \dot{E}'_q &= \left(-E_q + E_{fd}\right)/T'_{do} \\ \dot{E}_{fd} &= -\frac{1}{T_A} E_{fd} + \frac{K_A}{T_A}\left(V_{s0} - V_s\right) \end{aligned} \qquad (4)$$

Where V_s, V_{so} are the terminal voltage and the reference of terminal voltage respectively and also,

$$\begin{aligned} &T_e = P_e = V_{sq} I_q + V_{sd} I_d, E_q = E'_q + \left(X_d - X'_d\right) I_d, \\ &V_s = \sqrt{V_{sd}^2 + V_{sq}^2}, V_{sd} = X_q I_q, V_{sq} = E'_q - X'_d I_d, \\ &I_d = I_{1d} + I_{2d} + I_{3d}, I_q = I_{1q} + I_{2q} + I_{3q} \end{aligned} \qquad (5)$$

From Fig. 1 we can have,

$$V_s = jX_s I_s + j\left(X_{L1} + X_{t1}\right) I_1 - V_{i1} + V_b \qquad (6)$$

$$j\left(X_{L1} + X_{t1}\right) I_1 - V_{i1} = j\left(X_{L2} + X_{t2}\right) I_2 - V_{i2} \qquad (7)$$

$$j\left(X_{L3}\right) I_3 = j\left(X_{L1} + X_{t1}\right) I_1 - V_{i1} \qquad (8)$$

That is,

$$\begin{aligned} &V_{sd} + jV_{sq} = jX_s\left(I_{1d} + jI_{1q} + I_{2d} + jI_{2q} + I_{3d} + jI_{3q}\right) + \\ &j\left(X_{L1} + X_{t1}\right)\left(I_{1d} + jI_{1q}\right) - V_{i1d} - jV_{i1q} + V_b \sin\delta + jV_b \cos\delta \\ &= X_q\left(I_{1q} + I_{2q} + I_{3q}\right) + j\left[E'_q - X'_d\left(I_{1d} + I_{2d} + I_{3d}\right)\right] \end{aligned} \qquad (9)$$

$$\begin{aligned} &j\left(X_{L1} + X_{t1}\right)\left(I_{1d} + jI_{1q}\right) - V_{i1d} - jV_{i1q} \\ &= j\left(X_{L2} + X_{t2}\right)\left(I_{2d} + jI_{2q}\right) - V_{i2d} - jV_{i2q} \end{aligned} \qquad (10)$$

$$\begin{aligned} &j\left(X_{L3}\right)\left(I_{3d} + jI_{3q}\right) \\ &= j\left(X_{L1} + X_{t1}\right)\left(I_{1d} + jI_{1q}\right) - V_{i1d} - jV_{i1q} \end{aligned} \qquad (11)$$

From (1-11), we can obtain,

$$I_{1q} = V_{i1d} X_{q11} + V_{i2d} X_{q21} + V_b X_{qb1} \sin\delta \qquad (12)$$

$$I_{1d} = V_{i1q} X_{d11} + V_{i2d} X_{d21} + V_b X_{db1} \cos\delta + E'_q X_{de1} \qquad (13)$$

$$I_{2q} = V_{i1d} X_{q12} + V_{i2d} X_{q22} + V_b X_{qb2} \sin\delta \qquad (14)$$

$$I_{2d} = V_{i1q} X_{d12} + V_{i2d} X_{d22} + V_b X_{db2} \cos\delta + E'_q X_{de2} \qquad (15)$$

$$I_{3q} = V_{i1d} X_{q13} + V_{i2d} X_{q23} + V_b X_{qb3} \sin\delta \qquad (16)$$

$$I_{3d} = V_{i1q} X_{d13} + V_{i2d} X_{d23} + V_b X_{db3} \cos\delta + E'_q X_{de3} \qquad (17)$$

where the constants of (12-17), given in appendix B.

By linearizing the (4-17), we can obtain,

$$\begin{aligned} \Delta\dot{\delta} &= \omega_0 \Delta\omega \\ \Delta\dot{\omega} &= \left(-\Delta P_e - D\Delta\omega\right)/2H \\ \Delta\dot{E}'_q &= \left(-\Delta E_q + \Delta E_{fd}\right)/T'_{do} \\ \Delta\dot{E}_{fd} &= -\frac{1}{T_A}\Delta E_{fd} + \frac{K_A}{T_A}\Delta V_s \end{aligned} \qquad (18)$$

Where,

$$\begin{aligned} \Delta P_e &= K_1\Delta\delta + K_2\Delta E'_q + K_{pd}\Delta V_{dc} + K_{p1}\Delta m_1 \\ &+ K_{p\delta 1}\Delta\delta_1 + K_{p2}\Delta m_2 + K_{p\delta 2}\Delta\delta_2 \end{aligned} \qquad (19)$$

$$\begin{aligned} \Delta E'_q &= K_4\Delta\delta + K_3\Delta E'_q + K_{qd}\Delta V_{dc} + K_{q1}\Delta m_1 \\ &+ K_{q\delta 1}\Delta\delta_1 + K_{q2}\Delta m_2 + K_{q\delta 2}\Delta\delta_2 \end{aligned} \qquad (20)$$

$$\Delta V_s = K_5\Delta\delta + K_6\Delta E'_q + K_{vd}\Delta V_{dc} + K_{v1}\Delta m_1 + K_{v\delta 1}\Delta\delta_1 + K_{v2}\Delta m_2 + K_{v\delta 2}\Delta\delta_2 \quad (21)$$

$$\Delta V_{dc} = K_7\Delta\delta + K_8\Delta E'_q - K_9\Delta V_{dc} + K_{c1}\Delta m_1 + K_{c\delta 1}\Delta\delta_1 + K_{c2}\Delta m_2 + K_{c\delta 2}\Delta\delta_2 \quad (22)$$

By substituting (19-22) with (18), we can obtain the state variable equations of the power system installed with the IPFC:

$$\begin{bmatrix}\Delta\dot{\delta}\\ \Delta\dot{\omega}\\ \Delta\dot{E}'_q\\ \Delta\dot{E}_{fd}\\ \Delta\dot{V}_{dc}\end{bmatrix} = \begin{bmatrix}0 & \omega_0 & 0 & 0 & 0\\ \frac{-K_1}{M} & \frac{-D}{M} & \frac{-K_2}{M} & 0 & \frac{-K_{pd}}{M}\\ \frac{-K_4}{T'_{d0}} & 0 & \frac{-K_3}{T'_{d0}} & \frac{1}{T'_{d0}} & \frac{-K_{qd}}{T'_{d0}}\\ \frac{K_A K_5}{T_A} & 0 & \frac{-K_A K_6}{T_A} & \frac{-1}{T_A} & \frac{-K_A K_{vd}}{T_A}\\ K_7 & 0 & K_8 & 0 & -K_9\end{bmatrix}\begin{bmatrix}\Delta\delta\\ \Delta\omega\\ \Delta E'_q\\ \Delta E_{fd}\\ \Delta V_{dc}\end{bmatrix} + \begin{bmatrix}0 & 0 & 0 & 0\\ \frac{-K_{p1}}{M} & \frac{-K_{p\delta 1}}{M} & \frac{-K_{p2}}{M} & \frac{-K_{p\delta 2}}{M}\\ \frac{-K_{q1}}{T'_{d0}} & \frac{-K_{q\delta 1}}{T'_{d0}} & \frac{-K_{q2}}{T'_{d0}} & \frac{-K_{q\delta 2}}{T'_{d0}}\\ \frac{-K_A K_{v1}}{T_A} & \frac{-K_A K_{v\delta 1}}{T_A} & \frac{-K_A K_{v2}}{T_A} & \frac{-K_A K_{v\delta 2}}{T_A}\\ K_{c1} & K_{c\delta 1} & K_{c2} & K_{c\delta 2}\end{bmatrix}\begin{bmatrix}\Delta m_1\\ \Delta\delta_1\\ \Delta m_2\\ \Delta\delta_2\end{bmatrix} \quad (23)$$

Where $\Delta m_1, \Delta m_2, \Delta\delta_1, \Delta\delta_2$ represent the linearization of the input control signals of the IPFC. The linearized dynamic model of (23), can be shown by Figure 2, where only one input control signal is demonstrated, with u begins 1 $(\Delta u = \Delta m_1)$, 2 $(\Delta u = \Delta m_2)$, $\delta_1(\Delta u = \Delta\delta_1)$ or $\delta_2(\Delta u = \Delta\delta_2)$ and $[k_{pu}], [k_{vu}], [k_{qu}], [k_{cu}]$ are the row vectors as defined below,

$[k_{pu}] = [k_{p1} \quad k_{p\delta 1} \quad k_{p2} \quad k_{p\delta 2}]$, $[k_{vu}] = [k_{v1} \quad k_{v\delta 1} \quad k_{v2} \quad k_{v\delta 2}]$,

$[k_{qu}] = [k_{q1} \quad k_{q\delta 1} \quad k_{q2} \quad k_{q\delta 2}]$, $[k_{cu}] = [k_{c1} \quad k_{c\delta 1} \quad k_{c2} \quad k_{c\delta 2}]$

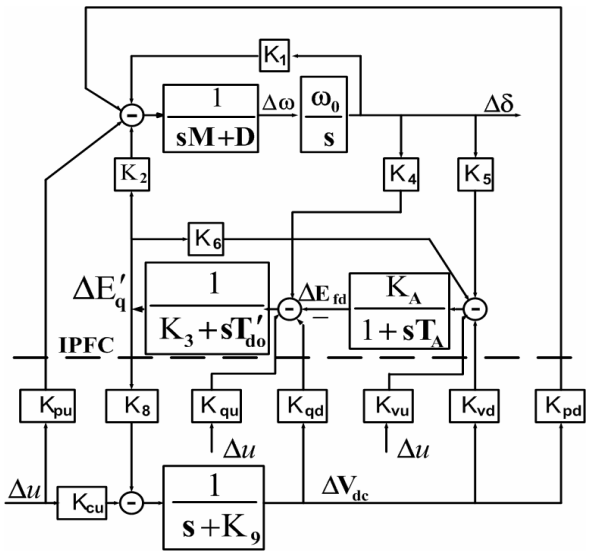

Figure 2. Proposed Philips-Heffron model of power system installed with IPFC.

From (23), it can be seen that there are four choices of input control signals of the IPFC to superimpose on the damping function of the IPFC, $m_1, m_2, \delta_1, \delta_2$. Therefore, in designing the damping controller of the IPFC, besides setting its parameters, the selection of the input control signal of the IPFC to superimpose on the damping function of the IPFC is also important.

IV. DESIGN OF DAMPING CONTROLLERS

The Philips-Heffron model of power system installed with IPFC (Fig. 2.) can be expressed with (24), that is obtained from (23), and shown in Figure 3, where H(s) and y are the transfer function of damping controller and feedback signal respectively. The (24) and Fig. 3, are the same as Larsen in [12] for TCSC and H. F. Wang in [10] for UPFC have expressed. The coefficients of (24), and transfer functions of (25) have been mentioned in [12].

$$\begin{bmatrix}\Delta\dot{\delta}\\ \Delta\dot{\omega}\\ \dot{\bar{x}}\end{bmatrix} = \begin{bmatrix}0 & \omega_b & 0\\ -k & -d & \bar{A}_{23}\\ \bar{A}_{31} & \bar{A}_{32} & \bar{A}_{33}\end{bmatrix}\begin{bmatrix}\Delta\delta\\ \Delta\omega\\ \bar{x}\end{bmatrix} + \begin{bmatrix}0\\ \bar{B}_2\\ \bar{B}_3\end{bmatrix}\Delta u_s \quad (24)$$

$$y = \begin{bmatrix}C_1 & C_2 & \bar{C}_3\end{bmatrix}\begin{bmatrix}\Delta\delta\\ \Delta\omega\\ \bar{x}\end{bmatrix}$$

And where,

$$K(s) = k + \frac{s}{\omega_b}d + \bar{A}_{23}^T\left(s\bar{I} - \bar{A}_{33}\right)^{-1}\left(\bar{A}_{31} + \frac{s}{\omega_b}\bar{A}_{32}\right)$$

$$K_0(s) = \left(\frac{\omega_b}{s}C_1 + C_2\right) + \bar{C}_3^T\left(s\bar{I} - \bar{A}_{33}\right)^{-1}\left(\frac{\omega_b}{s}\bar{A}_{31} + \bar{A}_{32}\right) \quad (25)$$

$$K_0(s) = \bar{A}_{23}^T\left(s\bar{I} - \bar{A}_{33}\right)^{-1}\bar{B}_3 + \bar{B}_2$$

$$K_{IL}(s) = \bar{C}_3^T\left(s\bar{I} - \bar{A}_{33}\right)^{-1}\bar{B}_3$$

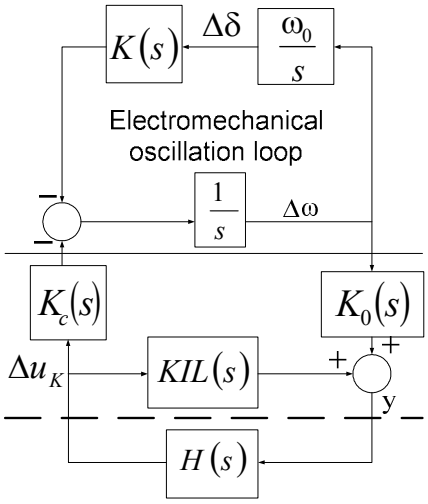

Figure 3. The closed loop system installed with IPFC damping controller.

We can obtain the electric torque provided by the IPFC damping controller to the electromechanical oscillation loop of the generator to be,

$$\Delta T_{IPFC} = \frac{K_c(\lambda_0)K_0(\lambda_0)H(\lambda_0)}{1 - K_{IL}(\lambda_0)H(\lambda_0)}\Delta\omega \quad (26)$$

where λ_0 is the angular frequency of system oscillation. A pure positive damping torque should be provided with an ideal IPFC damping controller to the electromechanical oscillation loop with $\Delta T_{IPFC} = D_{IPFC}\Delta\omega$, that is,

$$D_{IPFC} = \frac{K_c(\lambda_0)K_0(\lambda_0)H(\lambda_0)}{1-K_{IL}(\lambda_0)H(\lambda_0)} = [K_c(\lambda_0)K_0(\lambda_0)+D_{IPFC}K_{IL}(\lambda_0)]H(\lambda_0) = F(\lambda_0)H(\lambda_0) \quad (27)$$

F(λ_0) is named the forward path of the IPFC damping controller. Because of the variation of a F(λ_0) influence on the effectiveness of the IPFC damping controller, the magnitude of F(λ_0) can be used to analyze the effectiveness of the IPFC damping controller, the selection of power system operating condition at which the IPFC damping controller is designed and the choice of input control signals of the IPFC to be superimposed by the IPFC damping function. The criterion of the selection can be [10],

$$\mu_{selected} = \min_{\mu} F(\lambda_0, \mu, u_k), \quad \mu \in \Omega(\mu) \quad (28)$$

$$u_{selected} = \max_{u_k} F(\lambda_0, \mu_{selected}, u_k), \quad u_k \in \{m_1, m_2, \delta_1, \delta_2\} \quad (29a)$$

$$u_{selected} = \min_{u_k}\left[\max_{\mu} F(\lambda_0, \mu, u_k) - \min_{\mu} F(\lambda_0, \mu, u_k)\right], \quad u_k \in \{m_1, m_2, \delta_1, \delta_2\}, \mu \in \Omega(\mu) \quad (29b)$$

where $\Omega(\mu)$ is the set of the operating conditions of the power system that F(λ_0) is the function of system operating of the IPFC, μ and input control signal of the IPFC, u_k, $F(\lambda_0, \mu, u_k)$.

Equation (28) represents the IPFC damping control at the selected operating condition for design the damping controller should be haven least effective because of the robustness of the damping controller is achieved. To achieve the efficient of the IPFC damping function at minimum control cost the criterion of (29a), is applied. Equation (29b) is applied for a good design of damping controller to provide the steady damping overall the range of power system operating conditions, because:

(1) greatly increasing the damping contribution from the controller, the damping function with the variations power system operating conditions at some operating conditions could be too strong and pose much unwanted influence on other modes in the power system.

(2) a sharp drop on damping contribution from the controller with the variations power system operating conditions results in poor robustness.

Also (29b), must be applied jointly with (29a), not to fail the requirement of effectiveness.

After the choice of the suitable input control signal of the damping controller, we must design the controller function in order to damp the oscillation. The damping controllers are designed to produce an electrical torque in phase with the speed deviation. The four control parameters of the IPFC (i.e. $m_1, m_2, \delta_1, \delta_2$) can be modulated in order to produce the damping torque. The speed deviation $\Delta\omega$ is considered as the input to the damping controllers. The four alternative IPFC based damping controllers are examined in the present work. Damping controller based on IPFC control parameter m_1 shall henceforth be denoted as damping controller (m_1), similarly damping controllers based on m_2, δ_1, δ_2 shall henceforth be denoted as damping controller (m_2), damping controller (δ_1), and damping controller (δ_2), respectively.

The detailed step-by-step procedure for computing the parameters of the damping controllers using phase compensation technique is given below. In this paper a structure of IPFC based damping controller is,

$$H(s) = k_{dc}\left(\frac{s.T_\omega}{1+s.T_\omega}\right)\left(\frac{1+s.T_1}{1+s.T_2}\right) \quad (30)$$

1. Computation of natural frequency of oscillation ω_n from the mechanical loop.

$$\omega_n = \sqrt{\frac{K_1\omega_0}{M}} \quad (31)$$

K_1: the constant of model computed for operating condition and system parameters

ω_0 : frequency of operating condition (rad/sec)

ω_n :natural frequency of oscillation (rad/sec)

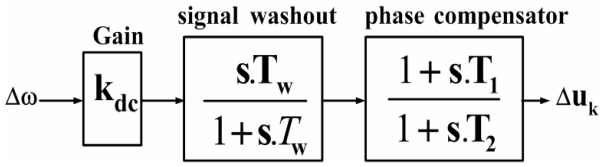

Figure 4. Structure of IPFC based damping controller.

2. Computation of $\angle GEPA$ (Phase lag between Δu and ΔP_e) at $s = j\omega_n$. Let it be γ.

3. Design of phase lead/lag compensator G_C :

The phase lead/lag compensator G_C is designed to provide the required degree of phase compensation. For 100% phase compensation,

$$\angle G_C(j\omega_n) + \angle GEPA\ (j\omega_n) = 0 \quad (32)$$

Assuming one lead-lag network, $T_1 = aT_2$, the transfer function of the phase compensator becomes,

$$G_C(s) = \frac{1+saT_2}{1+sT_2} \quad (33)$$

Since the phase angle compensated by the lead-lag network is equal to $-\gamma$, the parameters a and T_2 are computed as,

$$a = \frac{1+\sin(\gamma)}{1-\sin(\gamma)}, \quad T_2 = \frac{1}{\omega_n\sqrt{a}} \quad (34)$$

4. Computation of optimum gain K_{dc} .

The value of gain K_{dc} setting to achieve the required amount damping torque D_{IPFC} can be provided by IPFC damping controller.

The signal washout is the high pass filter that prevents steady changes in the speed from modifying the IPFC input parameter. The value of the washout time constant T_w should be high enough to allow signals associated with oscillations in rotor speed to pass unchanged. From the viewpoint of the washout function, the value of T_w is not critical and may be in the range of 1s to 20s. In this paper, T_w equal to 10s is chosen.

V. SIMULATION RESULTS

Parameters of an example single-machine infinite-bus power system have been shown by Fig. 1, and are given in the appendix A. The set of system operating conditions is,

$\Omega(\mu)$= {μ: V_{to} = 1.0 p.u., V_{bo} = 1.0 p.u., P_{eo} = 0.1 p.u. – 1.2 p.u.}

As it can be seen in Figure 5, the damping of the responsible electromechanical oscillation mode is negative or very poor over the set of system operating conditions and at the operating condition, μ_1 = {V_{to} = 1.0 p.u., V_{bo} = 1.0 p.u., P_{eo} = 1.2 p.u. } the oscillation mode is of the poorest damping.

In order to select the suitable damping signal, it has been used the result of calculation of the forward path over $\Omega(\mu)$ whose result to be superimposed to all the input control signals by the IPFC damping controller shown in Figure 6.

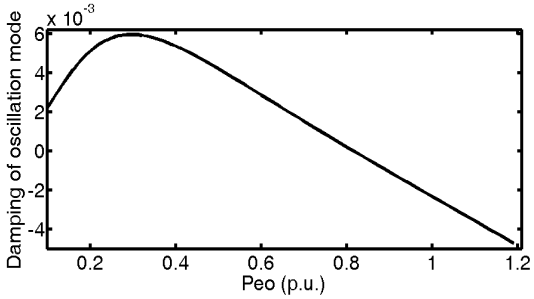

Figure 5. Damping of oscillation mode over $\Omega(\mu)$.

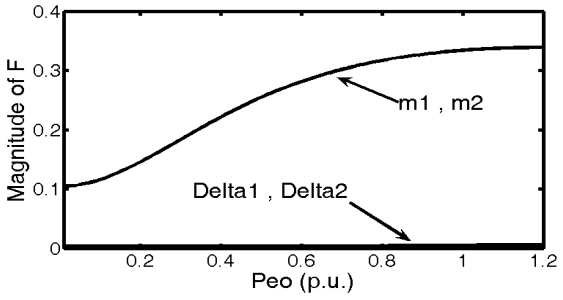

Figure 6. Variation of magnitude of F (λ_0) over $\Omega(\mu)$.

According to the criteria of (28), it can be seen that the operating condition to be selected for the design of the IPFC damping controller is:

μ_2 = {V_{to} = 1.0 p.u., V_{bo} = 1.0 p.u., P_{eo} = 0.1 p.u.}

At μ_2 , the most effective input control signals are $u_k = m_1, m_2$, as indicated in Fig. 6. So the criteria of (29a), lead to the selection of the input control signal for the IPFC damping controller as $u_k = m_1$ *or* m_2. The results of applying the criteria of (29b) for input control signal are:

(a) With $u_k = m_1, m_2$,

$$\frac{\max_{\mu} F(\lambda_0, \mu, u_k) - \min_{\mu} F(\lambda_0, \mu, u_k)}{\min_{\mu} F(\lambda_0, \mu, u_k)} = 2.25$$

(b) With $u_k = \delta_1, \delta_2$,

$$\frac{\max_{\mu} F(\lambda_0, \mu, u_k) - \min_{\mu} F(\lambda_0, \mu, u_k)}{\min_{\mu} F(\lambda_0, \mu, u_k)} = 6.37$$

Applying the criteria of (29a), (29b) shows that the damping controller with $u_k = \delta_1, \delta_2$ has not suitable damping torque to the electromechanical oscillation loop.

Therefore, with $u_k = m_1, m_2$, the IPFC damping controller provides the smoothest and suitable damping to the oscillation mode. Because once the IPFC damping controller is designed where providing a steady damping overall the range of power system operating conditions is our purpose, and $u_k = m_1, m_2$ is selected for the design of the controller.

The final result of the selection is:

μ_2 = {V_{to} = 1.0 p.u., V_{bo} = 1.0 p.u., P_{eo} = 0.1 p.u.}

$u_k = m_1$ *or* m_2

Then, the phase compensation method is used to set the parameters of the IPFC damping controller at μ_2 with $u_k = m_1$ *or* m_2. The results are,

With $u_k = m_1$,

K_{dc}= 19.55, T_w= 10 s, T_1= 0.08756s, T_2= 0.08763s.

With $u_k = m_2$,

Kdc= -19.55, T_w= 10 s, T_1= 0.08763s, T_2= 0.08756s.

The oscillation mode is moved by the IPFC damping controller with $u_k = m_1$ *or* m_2 to λ_0 = *-1.15 ± 11.3i* with a satisfactory damping around of 0.1.

It is used MATLAB/Simulnk software package for simulation to confirm the simple analysis above and demonstrate the damping controllers on power system oscillation stability where the power system and the IPFC are modeled by nonlinear differential equations of (1-4). However, the lead-lag controller is designed for the linearized system around the best operation condition. The oscillation once started to carry out a step load perturbation in mechanical power (i.e., $\Delta P_m = 0.01$ p.u.) and once to occur a three-phase to earth short circuit on the end of transmission line in the example power system at 1.0 second of the simulation and is cleared after 100 ms. For the analysis the dynamic responses of the system, we assumed that Master voltage source converter (VSC-M) injects active power to its line and Slave voltage source converter (VSC-S) absorbs active power from its line in any operating condition.

Because of similar operation of damping controllers based $u_k = m_1, m_2$ and only two of controller based $u_k = m_1$ is examined at operating condition μ_2 = (V_{to} = 1.0 p.u., V_{bo} = 1.0 p.u., P_{eo} = 0.1 p.u.), μ_1 = (V_{to} = 1.0 p.u., V_{bo} = 1.0 p.u., P_{eo} = 1.2 p.u.) and (V_{to} = 1.0 p.u., V_{bo} = 1.0 p.u., P_{eo} = 0.3 p.u.) and the phase compensation method is used to design the damping controller with two selection as shown in Table (1), where at μ_1 = {V_{to} = 1.0 p.u., V_{bo} = 1.0 p.u., P_{eo} = 1.2 p.u.} at which the oscillation mode has the poorest damping

when the power system installed no IPFC damping controller and $\mu_2 = \{V_{to} = 1.0$ p.u., $V_{bo} = 1.0$ p.u., $P_{eo} = 0.1$ p.u.$\}$ which by the criterion of the selection analysis is candid for design damping controller and $u_k = m_1$. Figures (7-14) show numerical results of nonlinear simulation with damping controller where 1: respective response at operating condition without damping controller, 2: respective response at operating condition with damping controller that designed at μ_1 with $u_k = m_1$, 3: respective response at operating condition with damping controller that designed at μ_2 with $u_k = m_1$,

TABLE. 1. RESULTS OF THE IPFC DAMPING CONTROLLER

Operating condition	Input control signal	Parameters of the IPFC damping controller	Electromechanical oscillation mode of the system
μ_1	$u_k = m_1$	$k_{dc} = 12.25$ $T_1 = 0.05101s$ $T_2 = 0.05093s$	$\lambda_0 = -1.99 \pm 19.5i$
μ_2	$u_k = m_1$	$k_{dc} = 19.55$ $T_1 = 0.08756s$ $T_2 = 0.08763s$	$\lambda_0 = -1.15 \pm 11.3i$

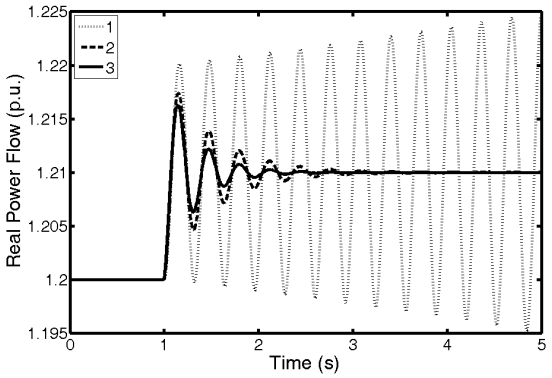

Figure 7. Power flow response at operating condition $\mu_1 = (V_{to} = 1.0$ p.u., $V_{bo} = 1.0$ p.u., $P_{eo} = 1.2$ p.u.) for $\Delta P_m = 0.01$ p.u

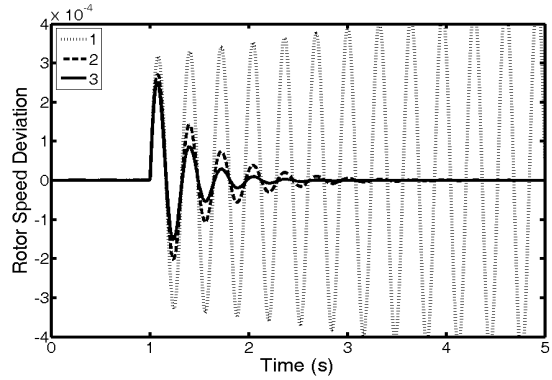

Figure 8. Rotor speed response at operating condition $\mu_1 = (V_{to} = 1.0$ p.u., $V_{bo} = 1.0$ p.u., $P_{eo} = 1.2$ p.u.) for $\Delta P_m = 0.01$ p.u.

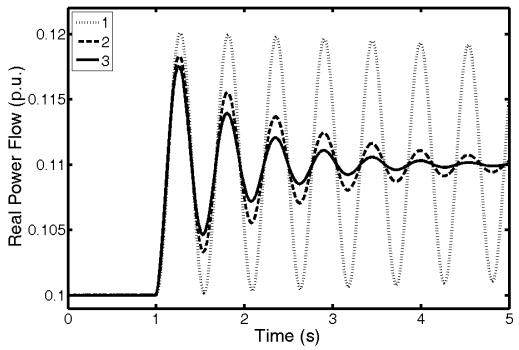

Figure 9. Power flow response at operating condition $\mu_2 = (V_{to} = 1.0$ p.u., $V_{bo} = 1.0$ p.u., $P_{eo} = 0.1$ p.u.) for $\Delta P_m = 0.01$ p.u.

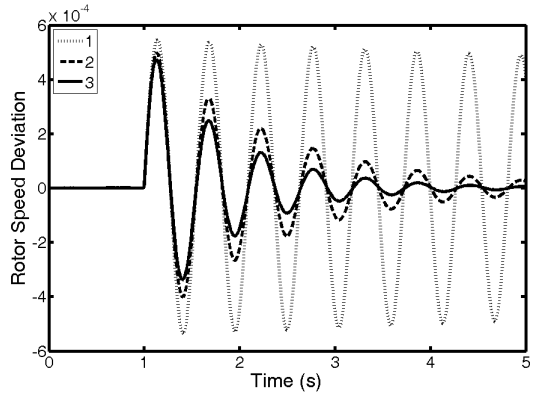

Figure 10. Rotor speed response at operating condition $\mu_2 = (V_{to} = 1.0$ p.u., $V_{bo} = 1.0$ p.u., $P_{eo} = 0.1$ p.u.) for $\Delta P_m = 0.01$ p.u.

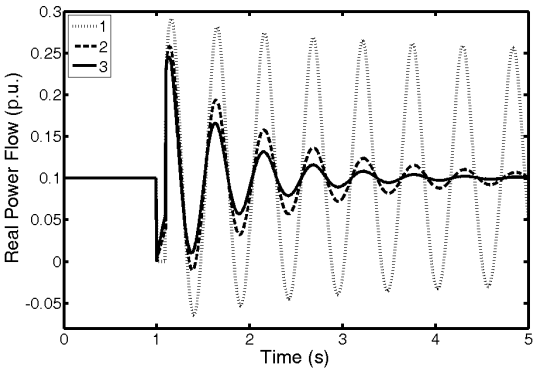

Figure 11. Power flow response at operating condition $\mu_2 = (V_{to} = 1.0$ p.u., $V_{bo} = 1.0$ p.u., $P_{eo} = 0.1$ p.u.) for a three-phase to earth short circuit.

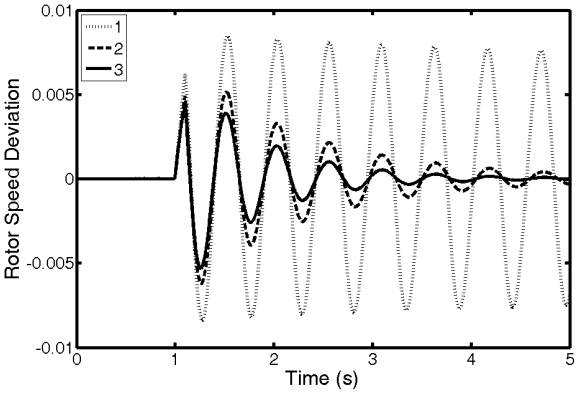

Figure 12. Rotor speed response at operating condition $\mu_2 = (V_{to} = 1.0$ p.u., $V_{bo} = 1.0$ p.u., $P_{eo} = 0.1$ p.u.) for a three-phase to earth short circuit.

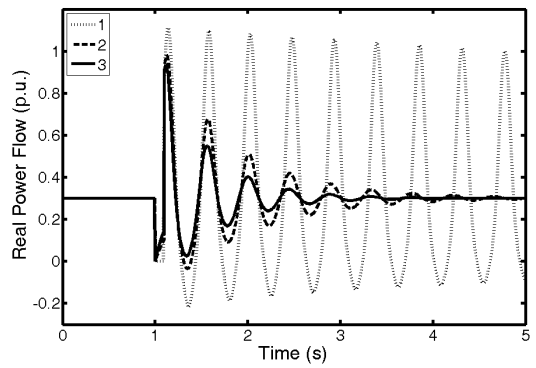

Figure 13. Power flow response at other operating condition (V_{to} = 1.0 p.u., V_{bo} = 1.0 p.u., P_{eo} = 0.3 p.u.) for a three-phase to earth short circuit.

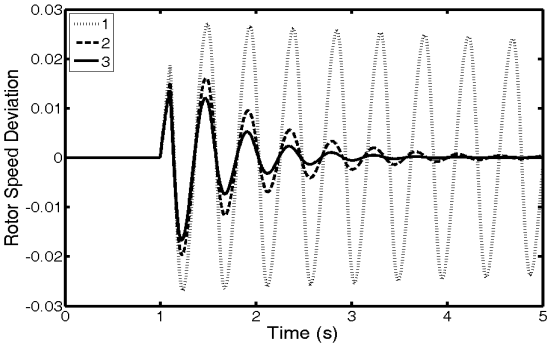

Figure 14. Rotor speed response at other operating condition (V_{to} = 1.0 p.u., V_{bo} = 1.0 p.u., P_{eo} = 0.3 p.u.) for a three-phase to earth short circuit.

It can be seen from Figures (7-14) that the IPFC damping controller set at μ_2 with $u_k = m_1$ is efficient and maintains both effectiveness and robustness at all load conditions for $\Delta P_m = 0.01$ p.u.. But the IPFC damping controller set at μ_2 with $u_k = m_1$ cannot suppress the oscillation when occurs a three-phase to earth short circuit only at higher loading of the power system. The IPFC damping controller set at μ_2 with $u_k = m_1$ is better than the IPFC damping controller set at μ_1 and provides a steady damping over the power system conditions above.

VI. CONCLUSION

In this paper the establishment of the linearized Phillips-Heffron model of a power system installed with an Interline Power Flow Controller (IPFC) has been presented. A damping controller based on the Phillips-Heffron model has been designed for enhancing dynamic stability in a power system. It can be seen, by analyzing contribution of pure positive damping torque of the damping controllers and the selection of the power system suitable operating condition for good design of the IPFC damping controller, signals m_1, m_2 based controllers have more effect on damping of oscillations and provide the almost steady damping over all power system conditions.

APPENDIX

A. Appendix A

Example of single-machine infinite-bus power system:

$$X_d = 1.8\ pu, X_q = 1.77\ pu, X'_d = 0.293\ pu,$$
$$H = 0.7988\ MJ/MVA, D = 0.00059338\ pu$$
$$, K_a = 10\ pu, T_a = 0.01\ s, X_s = 0.1\ pu,$$
$$X_{t1} = X_{t2} = 0.1\ pu, X_{L1} = X_{L2} = 0.3\ pu,$$
$$X_{L3} = 0.4\ pu, V_b = 1\ pu, V_s = 1\ pu,$$
$$V_{dc} = 2\,pu, C_{dc} = 1\ pu, \omega_0 = 2\,pi \times 60$$

B. Appendix B

$$X_{q1} = X_q + X_s + X_{L1} + X_{t1} + \frac{(X_q + X_s)(X_{L1} + X_{t1})}{X_{L2} + X_{t2}} + \frac{(X_q + X_s)(X_{L1} + X_{t1})}{X_{L3}},$$

$$X_{d1} = X'_d + X_s + X_{L1} + X_{t1} + \frac{(X'_d + X_s)(X_{L1} + X_{t1})}{X_{L2} + X_{t2}} + \frac{(X'_d + X_s)(X_{L1} + X_{t1})}{X_{L3}},$$

$$X_{q11} = \frac{1}{X_{q1}}\left(\frac{-(X_q + X_s)}{X_{L2} + X_{t2}} - \frac{(X_q + X_s)}{X_{L3}} - 1\right), X_{q21} = \frac{1}{X_{q1}}\left(\frac{(X_q + X_s)}{X_{L2} + X_{t2}}\right)$$

$$X_{qb1} = \frac{1}{X_{q1}}, X_{d11} = \frac{1}{X_{d1}}\left(\frac{(X'_d + X_s)}{X_{L2} + X_{t2}} + \frac{(X'_d + X_s)}{X_{L3}} + 1\right),$$

$$X_{d21} = \frac{1}{X_{d1}}\left(\frac{-(X'_d + X_s)}{X_{L2} + X_{t2}}\right), X_{db1} = \frac{-1}{X_{d1}}, X_{de1} = \frac{1}{X_{d1}},$$

$$X_{q12} = \left[\left(\frac{X_{L1} + X_{t1}}{(X_{L2} + X_{t2})X_{q1}}\right)\left(\frac{-(X_q + X_s)}{X_{L2} + X_{t2}} - \frac{(X_q + X_s)}{X_{L3}} - 1\right) + \frac{1}{X_{L2} + X_{t2}}\right],$$

$$X_{q22} = \left[\left(\frac{X_{L1} + X_{t1}}{(X_{L2} + X_{t2})X_{q1}}\right)\left(\frac{(X_q + X_s)}{X_{L2} + X_{t2}}\right) - \frac{1}{X_{L2} + X_{t2}}\right],$$

$$X_{d12} = \left[\left(\frac{X_{L1} + X_{t1}}{(X_{L2} + X_{t2})X_{d1}}\right)\left(\frac{X'_d + X_s}{X_{L2} + X_{t2}} + \frac{X'_d + X_s}{X_{L3}} + 1\right) + \frac{-1}{X_{L2} + X_{t2}}\right],$$

$$X_{d22} = \left[\left(\frac{X_{L1} + X_{t1}}{(X_{L2} + X_{t2})X_{d1}}\right)\left(\frac{-(X'_d + X_s)}{X_{L2} + X_{t2}}\right) + \frac{1}{X_{L2} + X_{t2}}\right],$$

$$X_{db2} = -\left(\frac{X_{L1} + X_{t1}}{(X_{L2} + X_{t2})X_{d1}}\right), X_{de2} = \left(\frac{X_{L1} + X_{t1}}{(X_{L2} + X_{t2})X_{q1}}\right),$$

$$X_{q13} = \left[\left(\frac{X_{L1} + X_{t1}}{X_{L3}X_{q1}}\right)\left(\frac{-(X_q + X_s)}{X_{L2} + X_{t2}} - \frac{(X_q + X_s)}{X_{L3}} - 1\right) + \frac{1}{X_{L3}}\right]$$

$$X_{q23} = \left[\left(\frac{X_{L1} + X_{t1}}{X_{L3}X_{q1}}\right)\left(\frac{(X_q + X_s)}{X_{L2} + X_{t2}}\right)\right], X_{qb3} = \left(\frac{X_{L1} + X_{t1}}{X_{L3}X_{q1}}\right),$$

$$X_{d13} = \left[\left(\frac{X_{L1} + X_{t1}}{X_{L3}X_{d1}}\right)\left(\frac{X'_d + X_s}{X_{L2} + X_{t2}} + \frac{X'_d + X_s}{X_{L3}} + 1\right) - \frac{1}{X_{L3}}\right],$$

$$X_{d23} = \left[\left(\frac{X_{L1} + X_{t1}}{X_{L3}X_{d1}}\right)\left(\frac{-(X'_d + X_s)}{X_{L2} + X_{t2}}\right)\right], X_{db3} = -\left(\frac{X_{L1} + X_{t1}}{X_{L3}X_{d1}}\right),$$

$$X_{de3} = \left(\frac{X_{L1} + X_{t1}}{X_{L3}X_{d1}}\right), X_{qb2} = \left(\frac{X_{L1} + X_{t1}}{(X_{L2} + X_{t2})X_{q1}}\right),$$

REFERENCES

[1] A. R. Mahran, B. W. Hogg, and M. L. El-Sayed, "Co-ordinated control of synchronous generator excitation and static VAR compensator", IEEE Trans. Energy Conversion, Vol. 7, Issue 4, Dec. 1992, pp. 615-622.

[2] Li-Jun Cai and István Erlich, "Simultaneous coordinated tuning of PSS and FACTS damping controllers in large power systems", IEEE Transactions on Power Systems, Vol. 20, No. 1, February 2005, pp. 294-300.

[3] M. A. de Amorim, and F. D. Freitas, "Generator and FACTS devices supplementary controller settings for damping electromechanical oscillation in a long radial power system", IEEWPES Transmission & Distribution Conference & Exposition: Latin America, (2004), pp. 749-753.

[4] L. Gyugyi, K. K. Sen, C.D.Schauder, "The interline power flow controller concept: a new approach to power flow management in transmission systems", IEEE/PES Summer meeting, Paper No. PE316-PWRD-0-07-1998, San Diego, July 1998.

[5] Kazemi, A.; Karimi, E, "The effect of interline power flow controller (IPFC) on damping inter-area oscillations in the interconnected power systems", Industrial Electronics, 2006 IEEE International Symposium, Vol. 3, July 2006, pp. 1911 – 1915.

[6] L. Rouco, "Coordinated design of multiple controllers for damping power system oscillations", Elect. Power energy syst., Vol. 23, 2001, pp. 517-530.

[7] H.F. Wang, "Phillips-Heffron model of power systems installed with STATCOM and applications" IEE Proc. Generation, Transmission and Distribution, Vol. 149, Issue 6, pp. 659-666, Nov. 1999.

[8] H. F. Wang, "Unified model for the analysis of FACTS devices in damping power system oscillations-part III: unified power flow controller", IEEE Transactions on power delivery, Vol. 15, No. 3, July 2000, pp. 978-983.

[9] Ali T. Al-Awami, Y.L. Abdel-Magid, M.A. Abido, "A particle-swarm-based approach of power system stability enhancement with unified power flow controller", Electrical power and energy systems., Vol. 29, 2007, pp.251–259.

[10] H.F. Wang, "Damping function of unified power flow controller", IEE Proc.-Gener. transm. distrib. Vol. 146, No. 1, January 1999, pp.81-87.

[11] Nabavi-Niaki, A., and Iravam, M.R., "Steady-state and dynamic models of unified power flow controller (UPFC) for power system studies", IEEE Trans., 1996, PWRS-4, Vol. 11, pp. 1937-1943.

[12] Larsen, E.V., Sanchezgasca, J.J., and Chaw, J.H., "Concept for design of FACTS controllers to damp power swings", IEEE Trans., 1995, PWRS-2, Vol. 10, pp.948-956.